Inorganic Chemistry

Article

pubs.acs.org/IC

Coordination Structure Conversion of Hydrazone−Palladium(II) Complexes in the Solid State and in Solution

Fumi Kitamura,[†] Kana Sawaguchi,[‡] Asami Mori,[§] Shoji Takagi,[†] Takayoshi Suzuki,[§] Atsushi Kobayashi,[‡] Masako Kato,[‡] and Kiyohiko Nakajima*[,†]

[†]Department of Chemistry, Aichi University of Education, Kariya, Aichi 448-8542, Japan

[‡]Department of Chemistry, Faculty of Science, Hokkaido University, North-10 West-8 Kita-ku, Sapporo 060-0810, Japan

[§]Department of Chemistry, Faculty of Science, Okayama University, Okayama 700-8530, Japan

Supporting Information

ABSTRACT: We prepared hydrazone−palladium(II) complexes of $[PdCl_2(HL^n)]$ and $[PdCl(L^n)]$ (n = 1−3) by the reaction of $[PdCl_2(cod)]$ or $[PdCl_2(PhCN)_2]$ and the hydrazone ligands of HL^n {N'-(pyridin-2-ylmethylene)picolinohydrazide (HL^1), N'-[1-(pyridin-2-yl)ethylidene]picolinohydrazide (HL^2), and N'-[(6-methylpyridin-2-yl)methylene]picolinohydrazide (HL^3)}. The structures of the complexes were determined by X-ray analysis. The hydrazone ligands had κN(py1),κN(imine) and κN(amidate),κN(py2) bidentate coordination modes in $[PdCl_2(HL^n)]$ (**1**, n = 1; **2**, n = 2) and in $[PdCl_2(HL^3)]$ (**3**), respectively. In contrast, tridentate coordination modes of κN(py1),κN(imine),κN(py2) and κN(py1),κN(amidate),κN(py2) were observed in $[PdCl(L^n)]$ (**4**, n = 1; **5**, n = 2) and in $[PdCl(L^n)]$ (**6**, n = 1; **7**, n = 2; **8**, n = 3). Thermal conversion of complexes **1**−**3** to complexes **6**−**8** proceeded in acetonitrile. Complexes **4** and **5** were obtained from complexes **1** and **2**, respectively, in a basic acetonitrile solution under dark conditions. Complex **4** reverted immediately to complex **1** in an acidic acetonitrile solution that included hydrochloric acid. However, under room light, in the basic acetonitrile solution that included trimethylamine, complex **4** converted photochemically to complex **6**. The thermochromic or vapochromic structure conversion of these complexes also occurred in the solid state. On heating at 180 °C, the color of the crystals of complexes **1**, **2**, and **3** changed from yellow to orange in the solid state. ^{1}H NMR and/or UV−vis absorption spectroscopy confirmed that the orange complexes **6**−**8** were produced. The reddish-orange crystals of complexes **4** and **5** were exposed to hydrogen chloride vapor to yield the yellow products of complexes **1** and **2**, respectively.

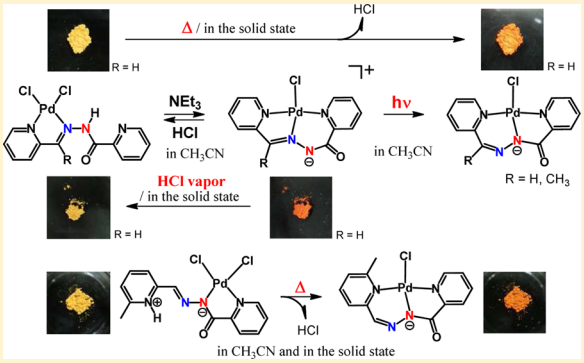

INTRODUCTION

We have focused our attention on chemical and physical stimuli-responsive transition-metal complexes in solution and in the solid state. Hydrazone compounds of the type $R^1R^2C{=}NNHR^3$ that have coordinating donor groups on R^n (n = 1−3) act as versatile ligands. A wide variety of hydrazone−metal complexes have been reported, and the structures and properties of the complexes have been investigated in efforts to explore their fascinating functionalities.[1−9] The catalytic capability,[10−14] biological application,[15−21] single-molecule magnet behavior,[22−24] and chromic behavior[2,25,26] of the complexes are some of the contemporary topics.

One of the characteristic properties of hydrazone−metal complexes is the high acidity of the H−N(amide) protons of hydrazone ligands that have κN(imine) coordination to metal ions. We have already investigated their acid−base behavior and reported that reversible protonation and deprotonation occurred on the coordinating hydrazone ligands in several metal complexes.[27−29] For example, the H−N(amide) proton of 2-(diphenylphosphino)benzaldehyde-2-pyridylhydrazone (HL) scarcely dissociates under basic conditions; however, the acid dissociation constant (pK_a) of $[PtCl(HL)]^+$ in methanol was found to be 6.7, and reversible deprotonation and protonation occurred smoothly upon the addition of small volumes of bases and acids.[27] A drastic change in color from yellow ($[PtCl(HL)]^+$) to red ($[PtCl(L)]$) was observed in acetonitrile upon the addition of a drop of triethylamine. The type of coordinating metal ion and the coordination geometry of the complexes strongly affect the degree of acidity of the H−N(amide) protons on the hydrazone ligands.

We reported previously that a hydrazone−copper(II) complex of [Cu(paph)Cl(MeOH)] {Hpaph = 2-[[2-(pyridin-2-yl)hydrazono]methyl]pyridine)} exhibits reversible protonation and deprotonation on the coordinating paph ligand.[28] The acid dissociation constant (pK_a) was determined to be 9.0 in methanol. [Cu(paph)Cl(MeOH)] showed colorful solvatochromism in various solvents of different polarities; however,

Received: May 19, 2015
Published: August 25, 2015

DOI: 10.1021/acs.inorgchem.5b01128
Inorg. Chem. 2015, 54, 8436−8448

the protonated form of $[Cu(Hpaph)Cl]^+$ displayed no solvatochromic behavior. Hence, we determined that deprotonation/protonation induced on−off switching of the solvatochromic behavior. Similar solvatochromic behavior was also observed in $[RuCl_2(PPh_3)_2(HL')]$ [HL′ = quinoline-2-carboxaldehyde (pyridine-2-carbonyl) hydrazone].[30] Moreover, we determined the vapochromic behavior of hydrogen-bonded proton-transfer assemblies composed of hydrazone−metal(II) complexes (metal M = Pd,[31] Fe[32]) and bromanilic acid or chloranilic acid and also the tribo-, thermo-, and vapochromic behavior of hydrazone−platinum(II) complexes[33] in the solid state. The chromic behavior of such hydrazone complexes induced by protonation/deprotonation requires further attention.

In those previous reports, protonation and deprotonation of the coordinated hydrazone ligands were consistently concerned with the chromic behavior of the complexes; however, their framework geometries around metals were basically not changed by protonation/deprotonation. Therefore, hydrazone complexes were used as building blocks to make up 1D, 2D, or 3D columns in hydrogen-bonded proton-transfer assemblies of platinum(II) and iron(II) complexes.

In this study, we focused on the coordination structure conversion of hydrazone−palladium(II) complexes induced by protonation/deprotonation and their related chromic behavior not only in solution but also in the solid state. The hydrazone compounds of HL^n {*N*′-(pyridin-2-ylmethylene)-picolinohydrazide (HL^1), *N*′-[1-(pyridin-2-yl)ethylidene]-picolinohydrazide (HL^2), and *N*′-[(6-methylpyridin-2-yl)-methylene]picolinohydrazide (HL^3); Scheme 1} can act as

Scheme 1. Hydrazone Ligands Used in This Study

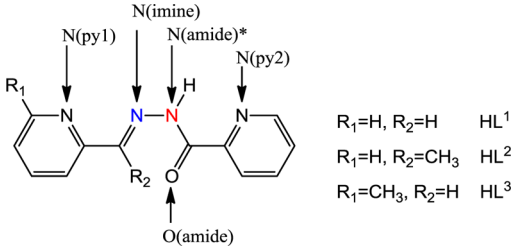

bidentate [κ*N*(py1),κ*N*(imine) or κ*N*(amidate),κ*N*(py2)] and tridentate [κ*N*(py1),κ*N*(imine),κ*N*(py2) or κ*N*(py1),κ*N*(amidate),κ*N*(py2)] ligands. We obtained various types of palladium(II) complexes, $[PdCl_2(HL^n)]$ and $[PdCl(L^n)]$, that have different coordination modes of the hydrazone ligands (Scheme 2). We successfully revealed the thermal and photochemical coordination structure conversion of these hydrazone complexes associated with a drastic change in color in solution and also their thermo- and vapochromic behavior in the solid state.

EXPERIMENTAL SECTION

General Procedures. ^1H NMR spectra were recorded on a Bruker AVANCE III NMR (400 MHz) spectrometer. UV−vis absorption spectra were obtained using a Shimadzu UV-1650PC or UV-2500PC spectrophotometer. For IR absorption measurements, samples were prepared by grinding powdered reagent with KBr, after which they were analyzed using a JASCO FT-IR 4100 spectrophotometer. Elemental analysis was conducted at the analysis center of Hokkaido University.

Synthesis of the Hydrazone Ligands. *N*′-(Pyridin-2-ylmethylene)picolinohydrazide (HL^1) was prepared by the reaction

Scheme 2. Schematic Representation of the Hydrazone−Palladium(II) Complexes

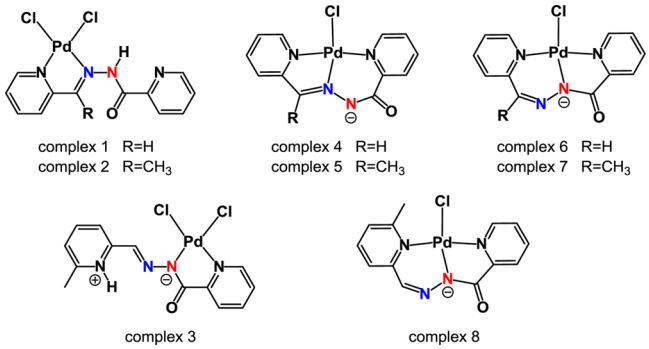

of 2-pyridinecarboxaldehyde and 2-pyridinecarboxylic acid hydrazide according to a reported procedure.[34] *N*′-[1-(Pyridin-2-yl)ethylidene]-picolinohydrazide (HL^2) and *N*′-[(6-methylpyridin-2-yl)methylene]-picolinohydrazide (HL^3) were similarly obtained as follows by the reaction of 2-acetylpyridine or 6-methylpyridinecarboxaldehyde with 2-pyridinecarboxylic acid hydrazide in ethanol, respectively.

Synthesis of HL^2. 2-Pyridinecarboxylic acid hydrazide (493.0 mg, 3.59 mmol) was added to a solution of 2-acetylpyridine (435.2 mg, 3.53 mmol) in ethanol (20 mL), and the reaction mixture was refluxed for 2 h. The solution was concentrated to a small amount under reduced pressure, and diethyl ether (6 mL) was added. A white microcrystalline precipitate of HL^2 formed, which was filtered and then dried in air. Yield: 781.0 mg, 90.5%. Anal. Calcd for HL^2 ($C_{13}H_{12}N_4O$): C, 64.99; H, 5.03; N, 23.32. Found: C, 65.07; H, 4.89; N, 23.37. ^1H NMR (chloroform-*d*) δ = 11.16 (s, 1H), 8.62 (t, *J* = 4.6 Hz, 2H), 8.39 (d, *J* = 8.0 Hz, 1H), 8.34 (d, *J* = 7.8 Hz, 1H), 7.92 (td, *J* = 7.7, 1.3 Hz, 1H), 7.74 (td, *J* = 7.6, 1.3 Hz, 1H), 7.52 (dd, *J* = 7.5, 4.8 Hz, 1H), 7.30 (dd, *J* = 7.3, 5.0 Hz, 1H), 2.59 (s, 3H).

Synthesis of HL^3. 2-Pyridinecarboxylic acid hydrazide (484.6 mg, 3.53 mmol) was added to a solution of 6-methylpyridinecarboxaldehyde (424.6 mg, 3.53 mmol) in ethanol (15 mL), and the reaction mixture was refluxed for 2 h. The solution was concentrated to a small amount under reduced pressure, and diethyl ether (6 mL) was added. A white microcrystalline precipitate of HL^3 formed, which was filtered and then dried in air. Yield: 821.1 mg, 96.8%. Anal. Calcd for HL^3 ($C_{13}H_{12}N_4O$): C, 64.99; H, 5.03; N, 23.32. Found: C, 64.94; H, 4.93; N, 23.24. ^1H NMR (chloroform-*d*) δ = 11.11 (s, 1H), 8.62 (d, *J* = 4.5 Hz, 1H), 8.33 (s, 1H), 8.32 (d, *J* = 7.6 Hz, 1H), 8.05 (d, *J* = 7.8 Hz, 1H), 7.92 (td, *J* = 9.0, 1.4 Hz, 1H), 7.65 (t, *J* = 7.7 Hz, 1H), 7.51 (dd, *J* = 7.1, 5.3 Hz, 1H), 7.17 (d, *J* = 7.6 Hz, 1H), 2.59 (s, 3H). A trace amount of the (*Z*)-isomer of HL^3 is included.

Synthesis of the Metal Complexes. $[PdCl_2(cod)]$[35] and $[PdCl_2(PhCN)_2]$[36] were prepared according to the published methods. ***Caution!*** *Complexes* ***1*****−****3** *are potentially not stable in solution and even in the solid state and converted gradually to complexes* ***6*** *and* ***7****. The basic acetonitrile solution of complexes* ***4*** *and* ***5*** *should be treated carefully in the dark. Otherwise, complexes* ***6*** *and* ***7*** *will be produced. Also, complexes* ***4*** *and* ***5*** *are thermally converted to complexes* ***6*** *and* ***7*** *even in the dark in an acidic acetonitrile solution.*

*Synthesis of [$PdCl_2${κN(py1),κN(imine)-HL^1}] (**1**).* The HL^1 ligand (55.5 mg, 0.245 mmol) was added to a solution of $[PdCl_2(cod)]$ (69.9 mg, 0.245 mmol) in acetonitrile (10 mL). The reaction mixture was allowed to stand for several hours at room temperature. Yellow needlelike crystals of complex **1** were obtained. The crystals were isolated by filtration and dried in air. Yield: 69.8 mg, 70.8%. Anal. Calcd for $[PdCl_2\{\kappa N(py1),\kappa N(imine)\text{-}HL^1\}]$ ($C_{12}H_{10}N_4OPdCl_2$): C, 35.71; H, 2.50; N, 13.88. Found: C, 35.56; H, 2.24; N, 13.74. ^1H NMR (acetonitrile-d_3): δ 12.58 (s, 1H), 9.91 (s, 1H), 9.06 (dd, *J* = 5.7 and 2.2 Hz, 1H), 8.68 (ddd, *J* = 4.8, 1.7, and 1.0 Hz, 1H), 8.15−8.22 (m, 2H), 7.98−8.07 (m, 2H), 7.63−7.72 (m, 3H). UV−vis [acetonitrile; λ_{max}, nm (log ε, M^{-1} cm^{-1})]: 217 (4.57), 272 (4.10), 300 (4.08), 331 (4.02), 365 (3.62, sh), 392 (3.15, sh). The filtrate was left for several days at room temperature to yield [PdCl-

DOI: 10.1021/acs.inorgchem.5b01128
Inorg. Chem. 2015, 54, 8436−8448

{κN(py1),κN(amidate),κN(py2)-L^1}] (**6**; to be described later). Yield: 17.3 mg, 19.2%.

*Synthesis of [PdCl$_2${κN(py1),κN(imine)-HL^2}] (**2**).* The HL^2 ligand (59.0 mg, 0.246 mmol) in acetonitrile (5 mL) was added to a solution of [PdCl$_2$(cod)] (70.2 mg, 0.246 mmol) in acetonitrile (2.5 mL). The reaction mixture was left to stand overnight at room temperature. Yellow platelike crystals of complex **2** were collected by filtration and dried in air. Yield: 47.6 mg, 46.3%. Anal. Calcd for [PdCl$_2${κN(py1),κN(imine)-HL^2}]·0.5H$_2$O ($C_{13}H_{13}N_4O_{1.5}PdCl_2$): C, 36.60; H, 3.07; N, 13.13. Found: C, 36.72; H, 3.09; N, 13.17. ^{1}H NMR (acetnitrile-d_3): δ 11.49 (s, 1H), 9.14 (ddd, *J* = 5.6, 1.5, and 0.5 Hz, 1H), 8.70 (ddd, *J* = 4.8, 1.6, and 0.9 Hz, 1H), 8.27 (td, *J* = 7.9 and 1.5 Hz, 1H), 8.15 (dt, *J* = 7.8 and 1.1 Hz, 1H), 7.96−8.08 (m, 2H), 7.78 (ddd, *J* = 7.8, 5.6, and 1.4 Hz, 1H), 7.66 (ddd, *J* = 7.6, 4.8, and 1.2 Hz, 1H), 2.47 (s, 3H). UV−vis [acetonitrile; λ_{max}, nm (log ε, M^{-1} cm^{-1})]: 216 (4.57), 269 (4.15), 312 (3.83, sh). The filtrate was left for several days at room temperature to yield a yellow precipitate of [PdCl{κN(py1),κN(amidate),κN(py2)-L^2}] (**7**; to be described later). Yield: 42.0 mg, 44.8%.

*Synthesis of [PdCl$_2$(κN(amidate),κN(py2)-HL^3)] (**3**).* The HL^3 ligand (48.2 mg, 0.201 mmol) was added to a solution of [PdCl$_2$(cod)] (57.2 mg, 0.200 mmol) in acetonitrile (5 mL). The reaction mixture was left to stand overnight at room temperature. A yellow microcrystalline precipitate of complex **3** formed. This was filtered and dried in air. Yield: 65.2 mg, 78.5%. Anal. Calcd for [PdCl$_2$(κN(amidate),κN(py2)-HL^3)] ($C_{13}H_{12}N_4OPdCl_2$): C, 37.39; H, 2.90; N, 13.42. Found: C, 36.87; H, 2.90; N, 13.16. The ^{1}H NMR spectrum of complex **3** was not recorded because of its poor solubility in various organic solvents. In order to measure the ^{1}H NMR spectrum, the crystal of complex **3** scarcely dissolving to water and various organic solvents was applied to dissolve in dimethyl sulfoxide (DMSO)-d_6 by heating, but it decomposed. UV−vis [acetonitrile; λ_{max}, nm (log ε, M^{-1} cm^{-1})]: 273 (3.93), 312 (3.75, sh), 408 (3.73). A precipitate of [PdCl{κN(py1),κN(amidate),κN(py2)-L^3}] (**8**; to be described later) was also obtained from the filtrate. Yield: 5.5 mg, 7.2%.

*Synthesis of [PdCl{κN(py1),κN(imine),κN(py2)-L^1}] (**4**).* **Method A:** The HL^1 ligand (39.6 mg, 0.175 mmol) in acetonitrile (10 mL) and triethylamine (17.8 mg, 0.176 mmol) was added to an acetonitrile solution (10 mL) of [PdCl$_2$(cod)] (50.6 mg, 0.177 mmol). The reaction mixture was left for several days in the dark at room temperature. Orange needlelike crystals of complex **4** formed. These were filtered and dried in air. Yield: 54.3 mg, 84.5%. **Method B:** Complex **4** was also prepared from [PdCl$_2$(PhCN)$_2$] instead of [PdCl$_2$(cod)] in a similar manner as follows. [PdCl$_2$(PhCN)$_2$] (38.3 mg, 0.100 mmol) was dissolved in acetonitrile (7 mL) containing triethylamine (11.5 mg, 0.110 mmol), and the HL^1 ligand (22.4 mg, 0.100 mmol) was added to the solution. The reaction mixture was stirred in the dark. An orange precipitate formed. This was filtered, washed with a small volume of dichloromethane, and dried in air. Yield: 30.6 mg, 83.0%. Anal. Calcd for [PdCl{κN(py1),κN(imine),κN(py2)-L^1}] ($C_{12}H_9N_4OPdCl$): C, 39.26; H, 2.47; N, 15.26. Found: C, 39.07; H, 2.42; N, 15.16. ^{1}H NMR (chloroform-*d*): δ 9.81 (dd, *J* = 6.0 and 2.0 Hz, 1H), 9.24 (dd, *J* = 5.8 and 2.0 Hz, 1H), 9.00 (dd, *J* = 8.0 and 2.4 Hz, 1H), 8.09 (td, *J* = 7.6 and 1.6 Hz, 1H), 7.96 (s, 1H), 7.92 (td, *J* = 7.7 and 1.5 Hz, 1H), 7.46−7.51 (m, 2H), 7.26 (td, *J* = 7.5 and 1.4 Hz, 1H). UV−vis [acetonitrile; λ_{max}, nm (log ε, M^{-1} cm^{-1})]: 219 (4.20, sh), 260 (3.97, sh), 284 (4.12), 306 (3.77, sh), 443 (3.95). **Method C:** Triethylamine (9.6 mg, 0.094 mmol) was added to an acetonitrile solution (8 mL) of complex **1** (20.0 mg, 0.050 mmol), and the solution was stirred in the dark at room temperature. An orange precipitate of [PdCl{κN(py1),κN(imine),κN(py2)-L^1}] formed. Yield: 12.0 mg, 65.4%.

*Synthesis of [PdCl{κN(py1),κN(imine),κN(py2)-L^2}] (**5**).* **Method A:** The HL^2 ligand (24.0 mg, 0.100 mmol) in acetonitrile (3 mL) and triethylamine (13.6 mg, 0.134 mmol) was added to an acetonitrile solution (2 mL) of [PdCl$_2$(cod)] (28.6 mg, 0.100 mmol). The reaction mixture was left overnight in the dark at room temperature. Orange needlelike crystals of complex **5** formed. These were filtered and dried in air. Yield: 16.2 mg, 42.5%. Anal. Calcd for [PdCl{κN(py1),κN(imine),κN(py2)-L^2}]·3H$_2$O ($C_{13}H_{17}N_4O_4PdCl$): C, 35.87; H, 3.94; N, 12.87. Found: C, 36.14; H, 3.77; N, 12.94. ^{1}H NMR (chloroform-*d*): δ 9.75 (dd, *J* = 5.9 and 1.5 Hz, 1H), 9.32 (ddd, *J* = 5.7, 1.4, and 0.5 Hz, 1H), 8.92 (dd, *J* = 8.0 and 1.8 Hz, 1H), 8.05 (td, *J* = 7.7 and 1.5 Hz, 1H), 7.95 (td, *J* = 7.8 and 1.6 Hz, 1H), 7.58 (ddd, *J* = 8.0, 1.2, and 0.6 Hz, 1H), 7.46 (ddd, *J* = 7.6, 6.0, and 1.8 Hz, 1H), 7.28 (ddd, *J* = 7.3, 5.8, and 1.3 Hz, 1H), 2.65 (s, 3H). UV−vis [acetonitrile; λ_{max}, nm (log ε, M^{-1} cm^{-1})]: 285 (4.21), 308 (3.94, sh), 442 (4.06). **Method B:** Complex **5** was also prepared in good yield from [PdCl$_2$(PhCN)$_2$] instead of [PdCl$_2$(cod)] in a similar manner as follows. [PdCl$_2$(PhCN)$_2$] (76.0 mg, 0.198 mmol) in acetonitrile (2 mL) was added to an acetonitrile solution (5 mL) of the HL^2 ligand (48.0 mg, 0.200 mmol) and triethylamine (20.8 mg, 0.206 mmol). The reaction mixture was left in the dark at room temperature. An orange precipitate formed immediately. This was filtered, washed with a small volume of dichloromethane, and dried in air. Yield: 67.6 mg, 89.6%. **Method C:** Triethylamine (2.5 mg, 0.025 mmol) was added to an acetonitrile solution (5 mL) of complex **2** (10.5 mg, 0.025 mmol). The solution was stirred in the dark at room temperature, to yield an orange precipitate. Yield: 6.4 mg, 67%.

*Synthesis of [PdCl{κN(py1),κN(amidate),κN(py2)-L^1}] (**6**).* **Method A:** Complex **1** (10.5 mg, 0.026 mmol) was dissolved in acetonitrile (20 mL) and refluxed for 7 h. The orange solution was concentrated to a small amount under reduced pressure, and diethyl ether (10 mL) was added. An orange microcrystalline precipitate of complex **6** formed, which was filtered and then dried in air. Yield: 5.8 mg, 60.9%. Anal. Calcd for [PdCl{κN(py1),κN(amidate),κN(py2)-L^1}] ($C_{12}H_9N_4OPdCl$): C, 39.26; H, 2.47; N, 15.26. Found: C, 39.04; H, 2.02; N, 15.12. ^{1}H NMR (chloroform-*d*): δ 10.03 (d, *J* = 5.9 Hz, 1H), 9.42 (d, *J* = 5.6 Hz, 1H), 8.20 (ddd, *J* = 7.8, 1.6, and 0.6 Hz, 1H), 8.05 (td, *J* = 7.6 and 1.5 Hz, 1H), 7.99 (td, *J* = 7.6 and 1.5 Hz, 1H), 7.52−7.58 (m, 2H), 7.50 (s, 1H), 7.34 (ddd, *J* = 7.7, 6.1, and 1.6 Hz, 1H). UV−vis [acetonitrile; λ_{max}, nm (log ε, M^{-1} cm^{-1})]: 252 (4.02), 277 (4.05), 405 (3.81), 444 (3.60, sh). **Method B:** Triethylamine (24.3 mg, 0.24 mmol) was added to a chloroform solution (30 mL) of complex **4** (30.1 mg, 0.082 mmol), and the reaction mixture was left for 2 weeks at room temperature under room light. The solution was concentrated, and a small volume of acetonitrile was added to yield an orange microcrystalline precipitate of complex **6**. Yield: 19.3 mg, 64.3%. The reaction also proceeded without an addition of a small volume of trimethylamine. Decomposition of complex **4** might occur in the presence of a large excess amount of triethylamine. **Method C:** Perchloric acid (6.2 mg, 0.062 mmol) was added to an acetonitrile solution (15 mL) of complex **4** (22.8 mg, 0.041 mmol). The solution was stirred overnight at room temperature to yield an orange microcrystalline precipitate of complex **6**. Yield: 12.2 mg, 81.3%.

*Synthesis of [PdCl{κN(py1),κN(amidate),κN(py2)-L^2}] (**7**).* **Method A:** Complex **2** (14.2 mg, 0.034 mmol) was dissolved in acetonitrile (13 mL) and refluxed overnight. The orange solution was concentrated to a small amount under reduced pressure, and diethyl ether (10 mL) was added. An orange microcrystalline precipitate of complex **7** formed. This was filtered and dried in air. Yield: 10.0 mg, 76.5%. Anal. Calcd for [PdCl{κN(py1),κN(amidate),κN(py2)-L^2}]·0.5H$_2$O ($C_{13}H_{12}N_4O_{1.5}PdCl$): C, 40.02; H, 3.10; N, 14.36. Found: C, 39.77; H, 3.25; N, 13.97. ^{1}H NMR (chloroform-*d*): δ 10.11 (dt, *J* = 6.0 and 1.1 Hz, 1H), 9.37 (ddd, *J* = 5.7, 1.4, and 0.6 Hz, 1H), 8.17 (ddd, *J* = 7.8, 1.6, and 0.6 Hz, 1H), 8.03 (td, *J* = 7.6 and 1.5 Hz, 1H), 8.00 (dd, *J* = 4.8 and 1.2 Hz, 2H), 7.52 (ddd, *J* = 7.4, 5.6, and 1.6 Hz, 1H), 7.34 (dt *J* = 5.8 and 4.4 Hz, 1H), 2.64 (s, 3H). UV−vis [acetonitrile; λ_{max}, nm (log ε, M^{-1} cm^{-1})]: 254 (4.07), 279 (4.10), 311 (3.72), 413 (3.76), 441 (3.69, sh). **Method B:** Triethylamine (97.2 mg, 0.961 mmol) was added to a dichloromethane solution (13 mL) of complex **5** (14.9 mg, 0.039 mmol). The reaction mixture was left for 2 weeks at room temperature under room light. The solution was concentrated, and a small volume of acetonitrile was added to yield an orange microcrystalline precipitate of complex **7**. Yield: 5.2 mg, 35%. **Method C:** Perchloric acid (2.1 mg, 0.20 mmol) was added to an acetonitrile solution (5 mL) of complex **5** (8.0 mg, 0.021 mmol). The solution was left for several days at room temperature to yield an orange microcrystalline precipitate of complex **7**. Yield: 4.6 mg, 60%.

DOI: 10.1021/acs.inorgchem.5b01128
Inorg. Chem. 2015, 54, 8436−8448

Table 1. Structural Parameters of Complexes 1·CH_3CN, 2·CH_3CN, 3·H_2O, 5·CH_3CN, 7·CH_3CN, and 8

	1·CH_3CN	2·CH_3CN	3·H_2O	5·CH_3CN	7·CH_3CN	8
Pd(1)−Cl(1)	2.279(1)	2.285(1)	2.310(1)	2.330(4)	2.336(2)	2.354(1)
Pd(1)−Cl(2)	2.279(1)	2.289(1)	2.311(1)			
Pd(1)−N(1)	2.026(3)	2.026(3)		2.032(11)	2.038(5)	2.040(2)
Pd(1)−N(2)	2.020(3)	2.008(3)		2.014(11)		
Pd(1)−N(3)			2.076(3)		1.962(6)	1.958(2)
Pd(1)−N(4)			2.027(2)	2.039(10)	2.040(5)	2.082(2)
O(1)−C(7)	1.209(4)	1.206(6)	1.229(4)	1.23(2)	1.193(9)	1.217(3)
N(2)−N(3)	1.372(4)	1.383(4)	1.372(4)	1.294(17)	1.283(10)	1.340(3)
N(2)−C(6)	1.281(5)	1.302(5)	1.253(5)	1.398(15)	1.317(10)	1.289(5)
N(3)−C(7)	1.364(5)	1.369(5)	1.364(3)	1.354(19)	1.466(9)	1.379(3)
Cl(1)−Pd(1)−Cl(2)	91.24(4)	91.42(4)	85.22(3)			
Cl(1)−Pd(1)−N(1)	95.10(4)	95.17(8)		91.8(4)	94.9(2)	94.76(7)
Cl(2)−Pd(1)−N(2)	93.95(9)	93.91(9)				
Cl(1)−Pd(1)−N(4)			92.93(9)	95.1(3)	92.0(1)	95.31(8)
Cl(2)−Pd(1)−N(3)			101.56(7)			
N(1)−Pd(1)−N(2)	79.70(11)	79.53(12)		82.0(5)		
N(1)−Pd(1)−N(3)					91.6(3)	89.39(10)
N(2)−Pd(1)−N(4)				91.2(5)		
N(3)−Pd(1)−N(4)			80.29(11)		81.5(3)	81.21(10)

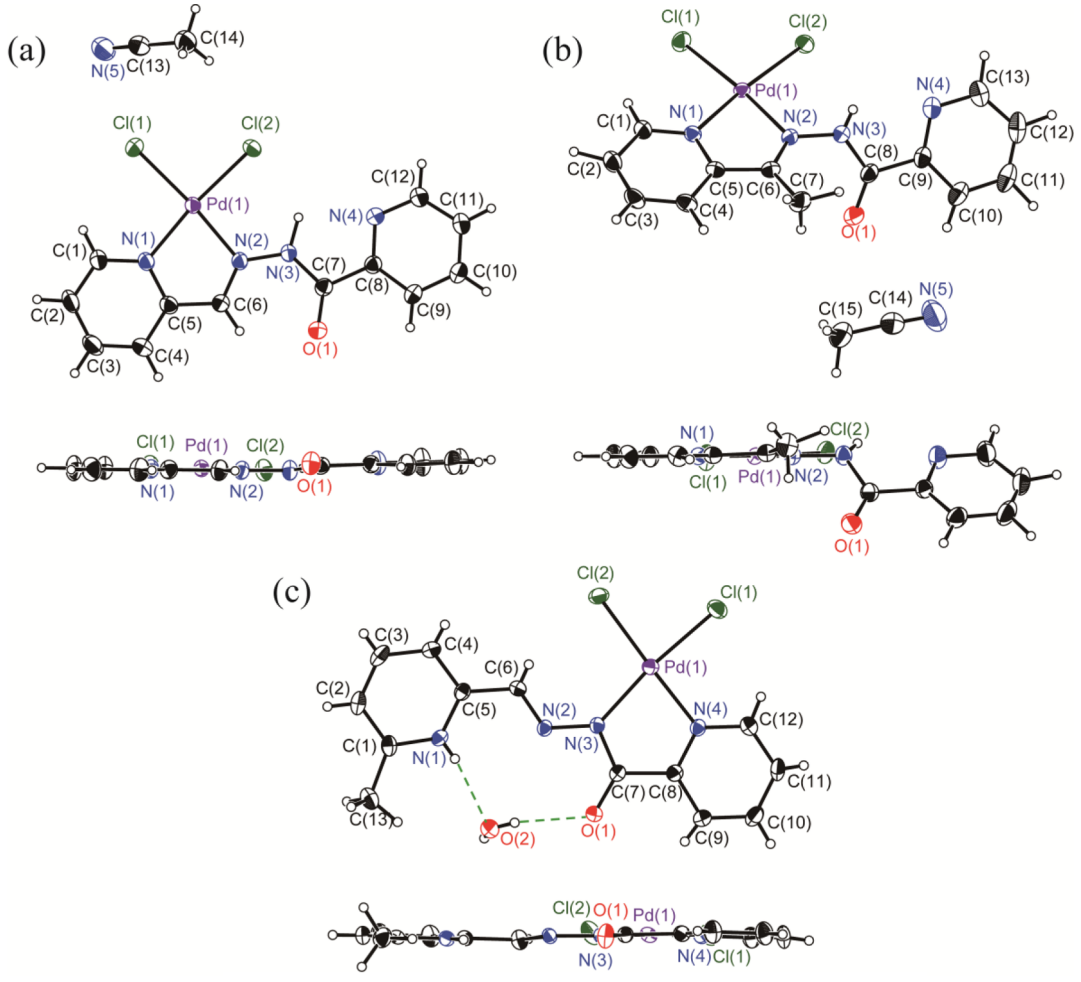

Figure 1. Perspective views of complexes with atom labeling schemes: (a) 1·CH_3CN; (b) 2·CH_3CN; (c) 3·H_2O.

*Synthesis of [PdCl{κN(py1),κN(amidate),κN(py2)-L^3}] (**8**).* **Method A:** Triethylamine (20.9 mg, 0.207 mmol) and the HL^3 ligand (53.8 mg, 0.224 mmol) were added to a solution of [$PdCl_2$(cod)] (57.0 mg, 0.200 mmol) in acetonitrile (5 mL) and left for several hours at room temperature. Orange needlelike crystals of complex **8** formed. The crystals were filtered and dried in air. Yield: 51.7 mg, 67.8%. Anal.

DOI: 10.1021/acs.inorgchem.5b01128
Inorg. Chem. 2015, 54, 8436−8448

Calcd for [PdCl{κN(py1),κN(amidate),κN(py2)-L^3}] ($C_{13}H_{11}N_4OPdCl$): C, 40.97; H, 2.91; N, 14.70. Found: C, 40.56; H, 3.04; N, 14.68. ^{1}H NMR (chloroform-*d*): δ 9.25 (ddd, *J* = 5.6, 1.4, and 0.6 Hz, 1H), 8.18 (ddd, *J* = 7.8, 1.5, and 0.6 Hz, 1H), 8.07 (td, *J* = 7.6 and 1.5 Hz, 1H), 7.81 (t, *J* = 7.6 Hz, 1H), 7.56 (ddd, *J* = 7.4, 5.6, and 1.6 Hz, 1H), 7.39 (d, *J* = 7.8 Hz, 1H), 7.30 (dd, *J* = 7.7 and 1.3 Hz, 1H), 7.28 (s, 1H), 3.28 (s, 3H). UV−vis [acetonitrile; λ_{max}, nm (log ε, M^{-1} cm^{-1})]: 255 (4.08), 280 (4.03), 337 (3.59, sh), 408 (3.84), 464 (3.53, sh). **Method B:** Complex **3** (10.3 mg, 0.025 mmol) was dissolved in acetonitrile (15 mL) and refluxed for several days. The orange solution was concentrated to a small amount under reduced pressure, and diethyl ether (10 mL) was added to yield an orange microcrystalline precipitate of complex **5**. This was filtered and dried in air. Yield: 7.2 mg, 76%.

Single-Crystal X-ray Diffraction Analysis. Single crystals of complexes **1**·CH_3CN, **2**·CH_3CN, **3**·H_2O, **5**·CH_3CN, **7**·CH_3CN, and **8** were obtained from their reaction mixtures by slow evaporation. Each single crystal was glued to the top of a glass fiber. X-ray diffraction data were obtained at ambient temperature using a Rigaku R-AXIS RAPID imaging-plate detector for complex **1**·CH_3CN and a Rigaku SCXmini CCD detector for complexes **2**·CH_3CN, **3**·H_2O, **5**·CH_3CN, **7**·CH_3CN, and **8** with graphite-monochromated Mo Kα radiation (λ = 0.71073 Å). The data were processed using the software package of *RAPID AUTO*[37] (for complex **1**·CH_3CN) or *CrystalClear*[38] (for complexes **2**·CH_3CN, **3**·H_2O, **5**·CH_3CN, **7**·CH_3CN, and **8**), and the numerical absorption corrections were applied. The structures were solved using direct methods employing *SIR2004*[39] or *SHELXS97*[40] and refined on F^2 (with all independent reflections) using *SHELXL97*.[40] All non-H atoms were refined anisotropically. All calculations were carried out using the software package of *CrystalStructure*.[41] Selected bond lengths and angles for complexes **1**·CH_3CN, **2**·CH_3CN, **3**·H_2O, **5**·CH_3CN, **7**·CH_3CN, and **8** are listed in Table 1, and the crystallographic data are shown in Table S1.

CCDC 1064016 (for complex **1**·CH_3CN), 1064017 (for complex **2**·CH_3CN), 1064018 (for complex **3**·H_2O), 1064019 (for complex **5**·CH_3CN), 1064020 (for complex **7**·CH_3CN), and 1064021 (for complex **8**) contain the supplementary crystallographic data for this paper. These data can be obtained free of charge from the Cambridge Crystallographic Data Center via www.ccdc.cam.ac.uk/data_request/cif.

Thermogravimetric (TG) Analysis. TG and differential thermal analysis were performed using a Rigaku ThermoEvo TG8120 analyzer (1 K min^{-1} heating; argon flow 300 mL min^{-1}).

RESULTS AND DISCUSSION

Preparation and Structural Characterization of Hydrazone−Palladium(II) Complexes. We successfully obtained hydrazone−palladium(II) complexes that have various types of ligand coordination modes (Scheme 2). Complexes **1**−**3** were easily prepared by mixing each hydrazone ligand (HL^n, *n* = 1−3) and [$PdCl_2$(cod)] in acetonitrile at room temperature, separately. The reaction mixture was allowed to stand for several hours, and single crystals of complexes **1**·CH_3CN, **2**·CH_3CN, and **3**·H_2O, suitable for X-ray structure determinations, precipitated.

Figure 1 displays perspective views of complexes **1**·CH_3CN, **2**·CH_3CN, and **3**·H_2O. The crystals of complexes **1**·CH_3CN, and **2**·CH_3CN include acetonitrile as a solvent molecule of crystallization. The crystal of complex **3**·H_2O contains a water molecule of crystallization. The geometry around the Pd atom is square-planar, and two chlorido ligands occupy positions cis to each other in complexes **1**−**3**. The ^{1}H NMR spectra of complexes **1** and **2** in CD_3CN show singlet resonances assigned to H−N(amide) protons at 12.58 (complex **1**) and 11.49 ppm (complex **2**), respectively. The coordinating hydrazone ligands of HL^1 and HL^2 have the same κN(py1),κN(imine) bidentate coordination mode around the Pd atom in complexes **1**·CH_3CN and **2**·CH_3CN. In contrast, a κN(amidate),κN(py2) bidentate coordination structure is observed in complex **3**·H_2O, and a water molecule of crystallization is hydrogen-bonded with O(1) and H−N(1) atoms in complex **3**·H_2O. A ^{1}H NMR spectrum of complex **3** was not available owing to its poor solubility in various organic solvents. It is worth noting that the coordinating HL^3 ligand in complex **3** exists as a zwitterion; that is, the coordinating N(3) [N(amidate)] is anionic, and the protonated N(1) [N(py1)] is cationic.

The O(1)−C(7) distance in complex **3**·H_2O [1.229(4) Å] is slightly longer than that in complexes **1**·CH_3CN and **2**·CH_3CN [1.209(4) and 1.206(6) Å, respectively], which is attributed to the conjugation of the π electrons on N(3) [N(amidate); N(3)···C(7)···O(1)]. The bidentate coordination of the hydrazone ligands forms planar five-membered chelate rings, and the bite angles of N(1)−Pd(1)−N(2) [**1**·CH_3CN, 79.70(11)°; **2**·CH_3CN, 79.53(12)°] and N(3)−Pd(1)−N(4) [**3**·H_2O. 80.29(11)°] are in a similar range. In complexes **1**·CH_3CN and **2**·CH_3CN, the bond angles of Cl(2)−Pd(1)−N(2) [93.95(9) and 93.91(9)°, respectively] are slightly smaller than those of Cl(1)−Pd(1)−N(1) [95.10(4) and 95.17(8)°, respectively]. The distance between Cl(2) and the proton H(1) attached to N(3) is 2.31(5) Å in complex **1**·CH_3CN and 2.72(5) Å in complex **2**·CH_3CN. These data suggest that there are hydrogen-bonding interactions between Cl(2) and the proton H(1) attached to N(3) in complexes **1**·CH_3CN and **2**·CH_3CN; however, the former interaction is notably stronger than the latter. In contrast, large bond angles of Cl(2)−Pd(1)−N(3) [101.56(7)°] are observed in complex **3**·H_2O, and the bond angles of Cl(1)−Pd(1)−Cl(2) [85.22(3)°] are notably smaller than those in complexes **1**·CH_3CN and **2**·CH_3CN [91.24(4) and 91.42(4)°, respectively]. This may be because the repulsion between Cl(2) and H−C(6) atoms enlarges the bond angles of Cl(2)−Pd(1)−N(3) and Pd(1)−N(3)−N(2) [135.2(2)°] and narrows the bond angle of Cl(1)−Pd(1)−Cl(2) in complex **3**·H_2O. Although no distinctive difference was observed in the Pd(1)−Cl(1) and Pd(1)−Cl(2) bond distances of complex **1**·CH_3CN [2.279(1) and 2.279(1) Å, respectively] and complex **2**·CH_3CN [2.285(1) and 2.289(1) Å, respectively], the bond distances of complex **3**·H_2O [2.310(1) and 2.311(1) Å, respectively] are comparatively longer. The trans influence of the κN(amidate),κN(py2) bidentate chelating ligand of HL^3 will be stronger than that of the HL^1 and HL^2 ligands with κN(py1),κN(imine) chelation because of the negative charge of N(3) [N(amidate)] that delocalized on the chelate ring. Therefore, it is assumed that elongation of the Pd(1)−Cl(1) and Pd(1)−Cl(2) bond distances took place in complex **3**·H_2O. Although the structures of the coordinating hydrazone ligands in complexes **1**·CH_3CN and **3**·H_2O are highly planar, the HL^2 ligand is twisted in complex **2**·CH_3CN. The torsion angle between the plane defined with N(1), N(2), and C(1)−C(6) and that with N(3), N(4), O(1), and C(8)−C(13) is 49.5(1)° in complex **2**·CH_3CN, which is caused by a steric repulsion between the methyl group [−C(7)H_3] and the O(1) atom, and this nonplanar geometry weakens the hydrogen-bonding interaction between the Cl(2) and H−N(3) atoms comparatively.

The single crystal of complex **5**·CH_3CN was obtained after the reaction mixture of the HL^2 ligand and [$PdCl_2$(cod)] was allowed to stand in a basic acetonitrile solution containing a small amount of trimethylamine for several days in the dark. The structure of complex **5**·CH_3CN was successfully determined by X-ray crystallographic analysis. Figure 2 displays

DOI: 10.1021/acs.inorgchem.5b01128
Inorg. Chem. 2015, 54, 8436−8448

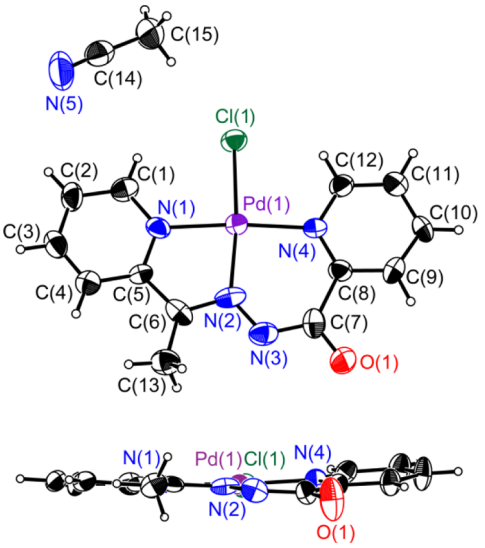

Figure 2. Perspective view of complex **5**·CH_3CN with an atom labeling scheme.

a perspective view of complex **5**·CH_3CN. The deprotonated $(L^2)^-$ ligand in complex **5**·CH_3CN has a κN(py1),κN(imine),κN(py2) tridentate coordination mode, and the coordination geometry around the Pd atom is square-planar.

The bond distances of N(2)−N(3) [1.29(2) Å] and N(3)−C(7) [1.35(2) Å] in complex **5**·CH_3CN are shorter than those [1.383(4) and 1.369(5) Å, respectively] observed in complex **2**·CH_3CN. In contrast, the bond distance of O(1)−C(7) [1.23(2) Å] in complex **5**·CH_3CN is longer than that [1.206(6) Å] confirmed in complex **2**·CH_3CN. It clearly shows that the C═O bond is weaker in complex **5**·CH_3CN. IR spectra of complexes **1**, **4**, and **6** and complexes **2**, **5**, and **7** were measured (Figure S1) The IR spectrum of complex **2** showed a characteristic C═O stretching vibration band at 1694 cm^{-1}; however, no strong IR absorption attributable to a C═O stretching vibration band of complex **5** was observed in the range of 1600−1700 cm^{-1}. Thus, it is suggested that deprotonation on the N(3) atom and tridentate chelation of the ligand caused a change in the π-conjugation state among the N(2), N(3), C(7), and O(1) atoms. Similar IR spectroscopic behavior was also observed for complexes **1** and **4**. A characteristic C═O stretching vibration band was observed at 1696 cm^{-1} in complex **1** but not in complex **4**.

We successfully obtained single crystals of complexes **7**·CH_3CN and **8** that were suitable for X-ray structural analysis directly from the reaction mixture upon standing, and we determined their structures. Parts a and b of Figure 3 show the molecular structures of complexes **7**·CH_3CN and **8**, respectively. The crystal of complex **7**·CH_3CN contains acetonitrile as solvent molecules of crystallization. Complexes **7**·CH_3CN and **8** have a similar κN(py1),κN(amidate),κN(py2) tridentate coordination mode of the deprotonated $(L^2)^-$ or $(L^3)^-$ ligand, which is different from the κN(py1),κN(imine),κN(py2) coordination mode of the $(L^2)^-$ ligand in complex **5**·CH_3CN. There are very few differences in the bond distances among these complexes. The bond distance of O(1)−C(7) in complex **7**·CH_3CN [1.193(9) Å] is somewhat shhorter than that in complex **2**·CH_3CN [1.206(6) Å], and the C═O stretching vibration band of complex **7** is observed at 1653 cm^{-1}.

Although the coordinating $(L^2)^-$ ligand is planar in complexes **5**·CH_3CN and **7**·CH_3CN, the $(L^3)^-$ ligand is bent in complex **8** in order to avoid the steric hindrance between Cl(1) and the methyl group [−C(13)H_3]. The folding angle between the least-squares plane of the Pd(1), Cl(1), N(3), N(4), O(1), and C(7)−C(12) set and that of the N(1)−N(3), C(1)−C(6), and C(13) set is 47.9(1)°.

Figure 4a shows UV−vis absorption spectra of complexes **1**−**3** in acetonitrile. Complex **3** shows an absorption band at 408 nm, but no absorption band was observed on this wavelength region for complexes **1** and **2**. Absorption bands were observed on the short-wavelength side at 331, 300, and 272 nm for complex **1** and at 312 and 269 nm for complex **2**. Thus, the UV−vis absorption spectra of complexes **1** and **2** are similar but differ from the spectrum of complex **3**. That is, it seems that the coordination structures of complexes **1** and **2** are similar, and they are different from that of complex **3** in acetonitrile. These spectral aspects are consistent with the result obtained by X-ray analysis that complex **3** has a κN(amidate),κN(py2) and complexes **1** and **2** have a κN(py1),κN(imine) bidentate coordination mode in each crystal.

Absorption bands were observed at 443 and 284 nm for complex **4** and at 442 and 285 nm for complex **5** (Figure 4b). The UV−vis absorption spectra of complexes **4** and **5** in acetonitrile thus closely resemble each other. We also measured

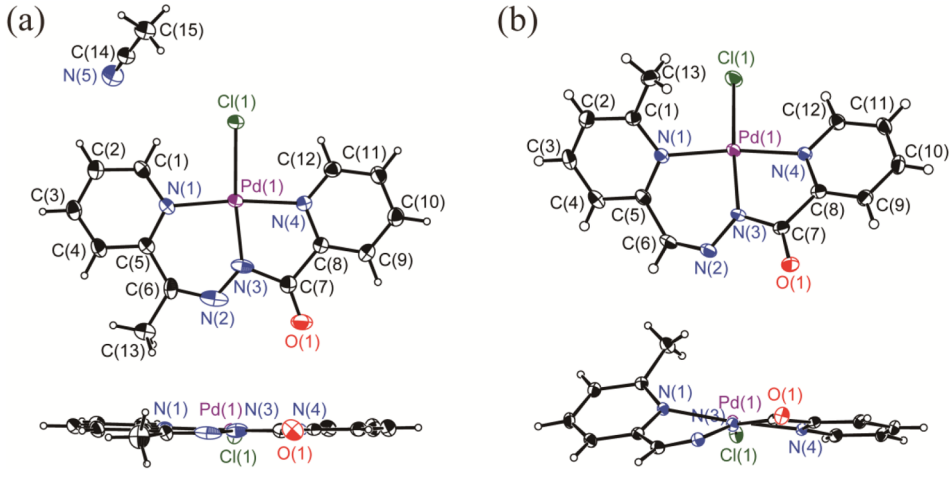

Figure 3. Perspective views of complexes with atom labeling schemes: (a) **7**·CH_3CN; (b) **8**.

DOI: 10.1021/acs.inorgchem.5b01128
Inorg. Chem. 2015, 54, 8436−8448

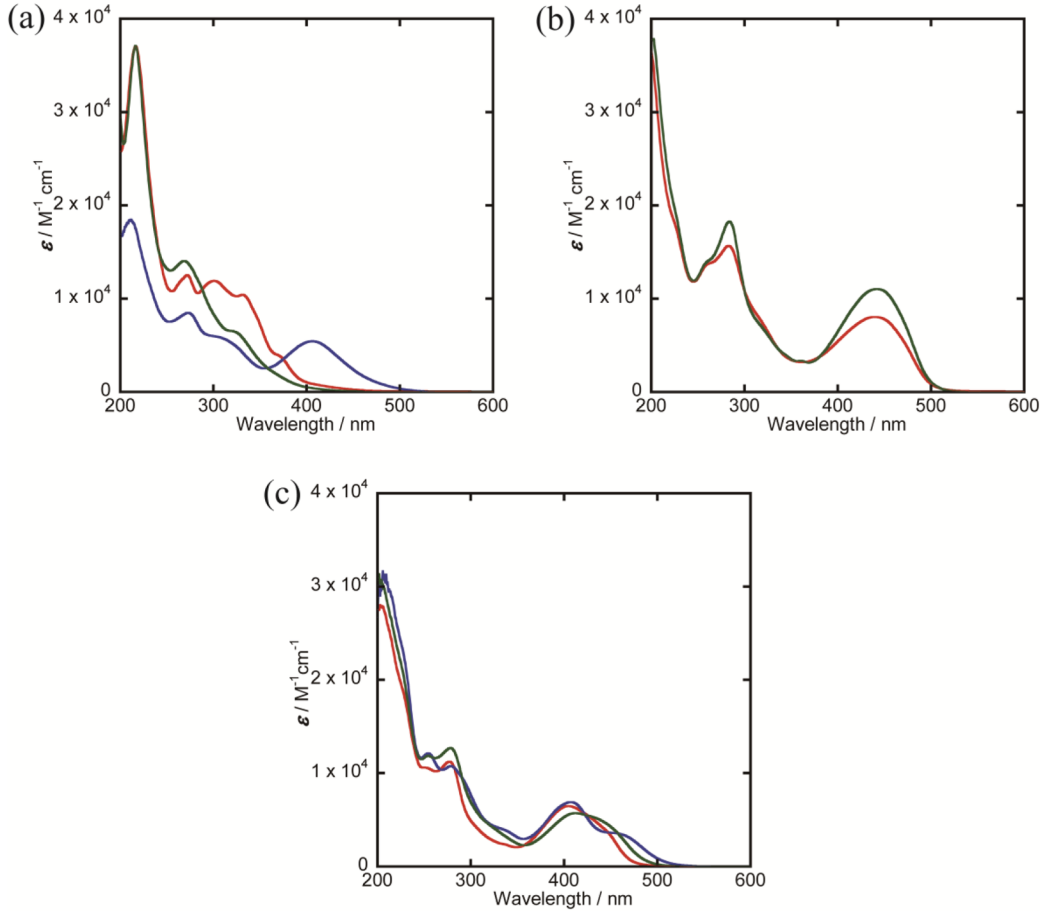

Figure 4. UV−vis absorption spectra of complexes in acetonitrile: (a) **1** (red line), **2** (green line), and **3** (blue line) [a small volume of hydrochloric acid was added to prevent deprotonation of H−N(amide)]; (b) **4** (red line) and **5** (green line); (c) **6** (red line), **7** (green line), and **8** (blue line).

the ^{1}H NMR spectra of complexes **4** and **5** in $CDCl_3$ (Figure S2). Singlet resonances of the methyl protons of complex **5** and of the imine proton of complex **4** were observed at 2.65 and 7.96 ppm, respectively. The ^{1}H NMR spectral aspects of the other resonances of eight protons on the two pyridine rings in complexes **4** and **5** are also quite similar. We therefore concluded that complex **4** also had a κN(py1),κN(imine),κN(py2) tridentate coordination mode of the deprotonated $(L^1)^-$ ligand, analogous to that of the $(L^2)^-$ ligand in complex **5**, as determined by X-ray analysis.

Figure 4c shows UV−vis absorption spectra of complexes **6**−**8** in acetonitrile. Broad absorption bands were observed in the visible region at 405 and 444 (sh) nm for complex **6**, at 413 and 441 (sh) nm for complex **7**, and at 408 and 464 (sh) nm for complex **8**. Although the splitting of the absorption band around 400−500 nm of complex **8** is larger than that in complexes **6** and **7**, the spectral aspects of these complexes resemble each other. The similar coordination structures of complexes **7** and **8** were confirmed by X-ray analysis. The ^{1}H NMR spectrum of complex **6** exhibited resonance patterns of the eight protons on the two pyridine rings similar to those of complex **7** (Figure S2). We therefore concluded that the coordination structure of complex **6** was analogous to the structures of complexes **7** and **8**.

Complexes **3** and **6**−**8**, which have a coordinating N(amidate) atom of the hydrazone ligand, showed absorption peaks around 405−413 nm, and complexes **4** and **5**, which have a noncoordinating N(amidate) atom, showed peaks on the long-wavelength side at 442 and 443 nm; however, no absorption peak was observed in this wavelength region in complexes **1** and **2**, which have a N(amide) atom. We applied the time-dependent dnesity functional theory calculation for complexes **5** and **7**. It was suggested that the absorption band in the visible region was mainly attributed to the intraligand $\pi-\pi^*$ transition of the coordinating hydrazone ligand (Figure S3) The related copper(II), nickel(II), and platinum(II) complexes containing the deprotonated anionic hydrazonato ligand 2-[2-(diphenylphosphino)benzylidene]-1-(pyridin-2-yl)hydrazin-1-ide showed a characteristic absorption band in the visible region (420−506 nm), which were also attributed to intraligand transition of the hydrazone ligand.[27,28]

Thermal and Photochemical Coordination Structure Conversion in Solution. Previously, copper(II) complexes containing similar hydrazone ligands of *N*′-[(pyridine-2-yl)-methylene]pyrazine-2-carbohydrazide were prepared, and three different forms of crystals that contain tetranuclear, 1D chiral chain, and 1D decker structures of the complexes were obtained.[8] A hydrazone ligand bridged two Cu atoms in the tetranuclear discrete complex. The ligand had κN(py1),κN(imine) coordination to one copper(II) and κN(py2),κN(amidate) coordination to the other copper(II). On the other hand, tridentate κN(py1),κN(amidate),κN(py2) coordination of the ligand was observed in the 1D chiral chain and 1D decker structures of the complexes. However, a tridentate κN(py1),κN(imine),κN(py2) coordination mode of the ligand (corresponding to the coordination mode of complexes **4** and **5** in

DOI: 10.1021/acs.inorgchem.5b01128
Inorg. Chem. 2015, 54, 8436−8448

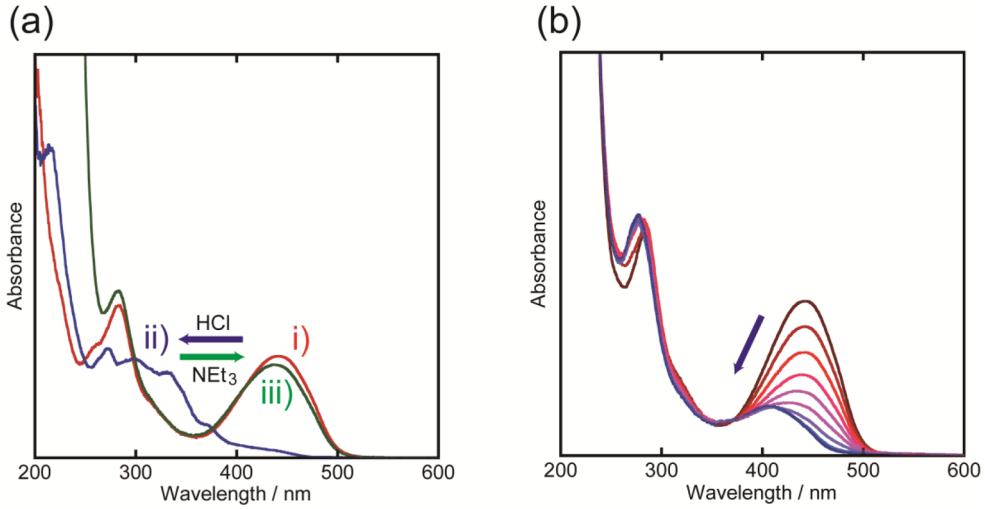

Figure 5. (a) UV−vis absorption spectra of complex **4** (i, red line) in acetonitrile, reaction solution **A** (ii, blue line) after a small volume of hydrochloric acid was added to the acetonitrile solution of complex **4** in the dark, and reaction solution **B** (iii, green line) after a drop of triethylamine was added to the solution **A** in the dark. The UV−vis absorption spectra of complex **4** changed to that of complex **1** upon the addition of a small volume of hydrochloric acid and reverted to that of complex **4** by the addition of a drop of triethylamine. (b) Change in the UV−vis absorption spectra of complex **4** in a basic acetonitrile solution that includes a small volume (1.68×10^{-3} M) of triethylamine at 30 min intervals under room light at ambient temperature. The UV−vis absorption spectra of complex **4** gradually changed to that of complex **6**.

Scheme 3. Acid−Base Equilibrium between Complexes 1 and 2 and Complexes 4 and 5 and the Plausible Mechanism for Photochemical Structure Conversion to Yield Complexes 6 and 7 in a Basic Acetonitrile Solution[a]

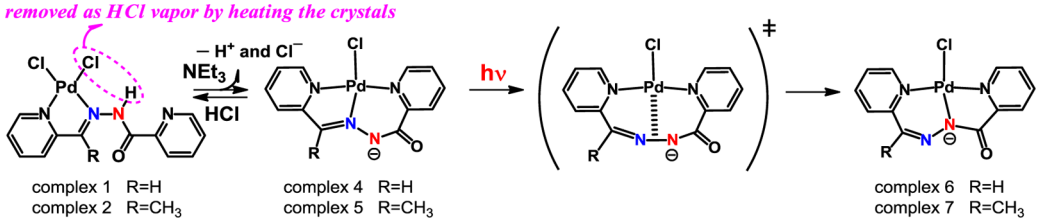

[a]The reaction from complexes **4** and **5** to complexes **6** and **7** does not proceed in the dark.

this work) was not observed, and the possible coordination structure conversion of the ligand was not mentioned.

Hydrazone ligands (HL^n, n = 1−3) are not colored, and the change in the color of the ligands was not observed in acetonitrile upon the addition of a small volume of triethylamine or hydrochloric acid. The acidity of the H−N(amide) protons of HL^n (n = 1−3) ligands is very low, and deprotonation hardly occurs in a basic acetonitrile solution. On the other hand, the color of the acetonitrile solution of complex **1** instantly changed from yellow to orange upon the addition of triethylamine, and complex **4** was obtained after the reaction mixture was left to stand under dark conditions (see the Experimental Section). Thus, deprotonation of H−N(amide) and structure conversion of the coordinating HL^1 ligand from bidentate to tridentate chelation proceeded smoothly in a basic acetonitrile solution. The UV−vis absorption spectrum of complex **4** in acetonitrile changed to that of complex **1** upon the addition of a small volume of hydrochloric acid in the dark (Figure 5a). The absorption spectrum of complex **1** immediately reverted to that of complex **4** by the addition of a drop of triethylamine. The structure conversion reactions between complexes **1** and **4** occurred reversibly in the dark.

The UV−vis absorption spectrum of complex **4** in a basic acetonitrile solution that included a small volume of triethylamine remained unchanged not only at ambient temperature but also at 60 °C in the dark (Figure S4); however, it gradually changed to that of complex **6** under room light at ambient temperature (Figure 5b). We actually isolated the crystals of complex **6** by standing the basic acetonitrile solution of complex **4** under room light for several days. Thus, the structure conversion of complex **4** in a basic acetonitrile solution proceeds photochemically under room light to yield complex **6**. Similar structure conversions of complex **2** also occurred, and complexes **5** and **7** were successfully prepared in a stepwise fashion. A plausible mechanism for such a photochemical conversion of coordination structures in these complexes is summarized in Scheme 3. Coordination structure conversion of the hydrazone ligands from bidentate κN(py1),-κN(imine) (complexes **1** and **2**) to tridentate κN(py1),κN(imine),κN(py2) (complexes **4** and **5**) coordination mode and photochemical *E*-to-*Z* isomerization of the −C═N− moiety of the coordinating $(L^n)^-$ (n = 1, 2) ligand and the following κN(imine) to κN(amidate) transformation would occur in a stepwise fashion at ambient temperature during the course of the reaction.

Although the UV−vis absorption spectrum of the acidic acetonitrile solution of complex **1** hardly changed either in the dark or under room light at ambient temperature, it gradually changed at 60 °C. Figure 6 shows the change in the UV−vis absorption spectrum of complex **1** in an acidic acetonitrile solution that includes a small volume of hydrochloric acid at 60

DOI: 10.1021/acs.inorgchem.5b01128
Inorg. Chem. 2015, 54, 8436−8448

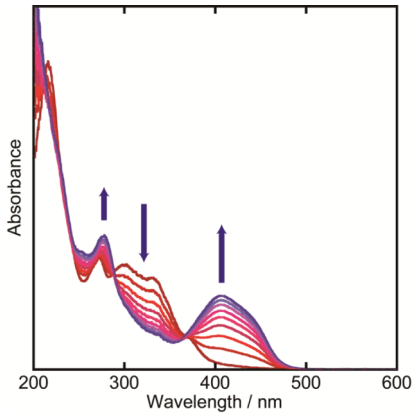

Figure 6. Change in the UV−vis absorption spectrum of complex **1** in an acidic acetonitrile solution that includes hydrochloric acid (8.6×10^{-4} M) at 4 h intervals in the dark at 60 °C. Hydrochloric acid was added to prevent deprotonation of H−N(amide) on the coordinated hydrazone ligand in complex **1**. The UV−vis absorption spectra of the complex (red line) changed gradually to that of complex **6** (blue line).

°C in the dark. The absorption bands at 300 and 331 nm gradually diminished over time, and a new absorption band appeared at 405 nm [444 (sh)]. Isosbestic points were retained at 289 and 367 nm throughout the reaction, and the converged spectrum was identical with that of complex **6**. In fact, complex **6** was prepared from complex **1** in acetonitrile by heating (as described in the Experimental Section). We concluded that the reaction proceeded thermally, as shown in Scheme 4. That is, complex **1** will get converted thermally to the intermediate complex cation of $[PdCl\{\kappa N(py1),\kappa N(imine),\kappa N(py2)\text{-}HL^1\}]^+$ [**A** in Scheme 4], which contains tridentate protonated hydrazone ligands in the $\kappa N(py1),\kappa N(imine),\kappa N(py2)$ mode. We were unable to isolate the unstable intermediate complex cation. The following $\kappa N(imine)$ to $\kappa N(amide)$ transformation and deprotonation of H−N(amide) will occur rapidly to yield complex **6**. It is intriguing that deprotonation of H−N(amide) occurs in the reaction process to yield complex **6** even in an acidic acetonitrile solution. However, the high acidity of the coordinating HL^1 ligand is sufficiently predictable on the basis of our previous data. We were also able to obtain complex **6** by the addition of a small volume of perchloric acid to the acetonitrile solution of complex **4** (see the Experimental Section for the synthesis of complex **6**, Method C). It is anticipated that protonation on the N(amidate) atom of the coordinated $(L^1)^-$ ligand in complex **4** would produce an intermediate complex cation (**A**) as shown in Scheme 4. The following thermal $\kappa N(imine)$ to $\kappa N(amidate)$ transformation reaction would then proceed to yield complex **6**. Complexes **6** and **7** are thermodynamically stable in an acetonitrile solution, and the reverse reaction from complexes **6** and **7** to complexes **1** and **2** did not occur.

It is of note that there are two pathways for the conversion of complex **1** to **6** and of complex **2** to **7** in acetonitrile; the reaction proceeds thermally in a slightly acidic acetonitrile solution (Scheme 4) and photochemically via complex **4** or **5** in a basic acetonitrile solution (Scheme 3).

Complex **8** was easily obtained from the acetonitrile solution of complex **3** by heating. It is clear that deprotonation of the bidentate HL^3 ligand in complex **3** enhances the substitution reaction of coordinating Cl^- by the N(py1) atom of the $(L^3)^-$ ligand to yield complex **8** (Scheme 5). The change in the absorption spectrum of complex **3** in acetonitrile was measured at ambient temperature in the dark (Figure 7). The final spectrum was similar to that of complex **8** after the reaction

Scheme 5. Facile Thermal Structure Conversion of Complex 3 in Acetonitrile[a]

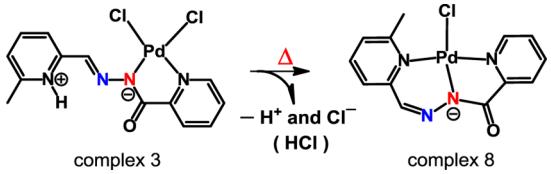

[a]Complex **8** is readily produced.

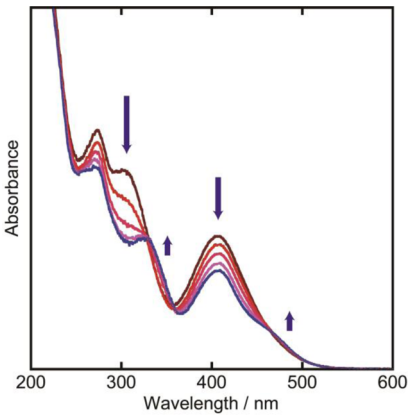

Figure 7. Change in the UV−vis absorption spectrum of complex **3** in acetonitrile at 1 h intervals in the dark at ambient temperature. The UV−vis absorption spectrum of complex **3** (brown line) changed gradually. The final spectrum (blue line) was similar to that of complex **8**.

Scheme 4. Plausible Mechanism for Thermal Structure Conversion of Complexes 1 and 2 in a Slightly Acidic Acetonitrile Solution To Yield Complexes 6 and 7[a]

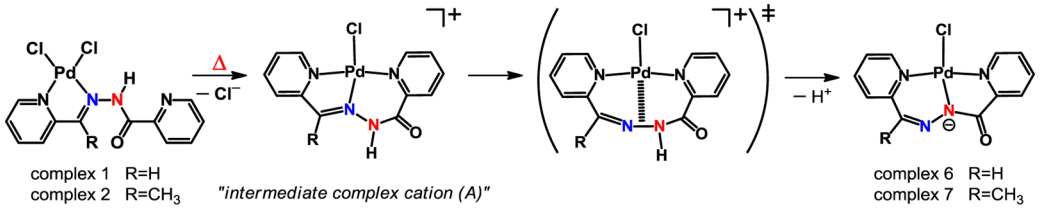

[a]The intermediate complex cation of $[PdCl\{\kappa N(py1),\kappa N(imine),\kappa N(py2)\text{-}HL^1\}]^+$ (**A**) was produced at first from complex **1** upon heating in an acidic acetonitrile solution, and the following $\kappa N(imine)$ to $\kappa N(amide)$ transformation and deprotonation of H−N(amide) occur to yield complex **6**.

DOI: 10.1021/acs.inorgchem.5b01128
Inorg. Chem. 2015, 54, 8436−8448

completed in ca. 4 h, and isosbestic points were retained at 328, 355, and 461 nm during the reaction time. It seems that deprotonation of H−N(py1), *E*-to-*Z* isomerization of the −C═N− moiety, elimination of the coordinating Cl^- ligand, and κN(py1) coordination to Pd proceed in succession. Although we added an excess amount of hydrochloric acid to the acetonitrile solution of complex **8**, we could not reproduce complex **3**.

It is well-known that azobenzenes and arylhydrazones undergo photoinduced *E*-to-*Z* isomerization, and the isomerization of arylhydrazones is reviewed.[42] In general, the thermodynamically stable form of azobenzenes and arylhydrazones is an *E* isomer.[43] It was reported that the *E* isomer of 2-[[2-(pyridin-2-yl)hydrazono]methyl]pyridine, *N*′-(pyridin-2-ylmethylene)benzohydrazide, and the related hydrazone ligands captured Zn^{2+} cation to yield stable zinc(II) complexes.[44] After the addition of a ligand of higher affinity for Zn^{2+} to the solution of zinc(II) complexes, the produced noncoordinating *E* isomer was converted to the *Z* isomer by photoirradiation. Moreover, the *E* isomer of *N*′-(pyridin-2-ylmethylene)-benzohydrazide captured K^+ cation, and the produced complex released K^+ cation by photoirradiation.[45] Then the *E* isomer was photochemically converted to the *Z* isomer.

Recently, the properties of (*E*)-*N*′-[1-(2-hydroxyphenyl)-ethylidene]isonicotinoylhydrazide and its metal complexes were reported in relation to their photoswitching character.[9] Photoinduced *E*-to-*Z* isomerization of arylhydrazones are well mentioned in the paper and the cited references. (*E*)-*N*′-[1-(2-Hydroxyphenyl)ethylidene]isonicotinoylhydrazide was photoisomerized to the *Z* isomer with UV light (λ = ∼400−315 nm) in solution and reverted to the original *E* isomer by UV-light irradiation (λ = 254 nm) or heating. The stable *E* isomer formed metal complexes with several di- and trivalent metal ions such as Cu^{2+}, Ni^{2+}, Al^{3+}, and Fe^{3+}; however, the *Z* isomer did not react with metal ions. The metal complexes including the *E* isomer were inert to photoreaction; that is, the *E* configuration of the coordinating hydorazone ligand was locked.

We successfully found out in this work that *E*-to-*Z* isomerization of the coordinating hydrazone ligands in complexes **3**−**5** occurred to yield complexes **6**−**8**, in which the coordinating hydrazone ligands were not released after isomerization.

Thermochromic and Vapochromic Coordination Structure Conversion in the Solid State. It was reported that the crystal structure conversion of the coordination polymers occurred by exposing a crystal of the copper(II) triazole complex to hydrogen chloride (HCl) vapor.[46] The 3D network of the copper(II) triazole complex was converted to a 1D chain structure. To the best of our knowledge, there are still very few reports on the structure conversion caused by exposing the crystals to acid/base vapor.

The change in color of the crystals of complex **1** from yellow to orange occurred when the crystals were heated at 180 °C for 1 h (Figure 8a). We prepared two samples of the products **A** (at 150 °C for 5 h) and **B** (at 180 °C for 1 h) by heating complex **1** in the solid state. Figure 9 shows ^{1}H NMR spectra of complexes **1**, **4**, and **6** and products **A** and **B**. ^{1}H NMR spectra of all of the complexes and products were measured in a $CDCl_3$ solvent. Considering the resonance patterns and intensities of the resonance peaks, it is obvious that product **A** is a mixture of complexes **4** and **6** in a 2:3 molar ratio. We confirmed that the UV−vis absorption spectra calculated for the mixture of

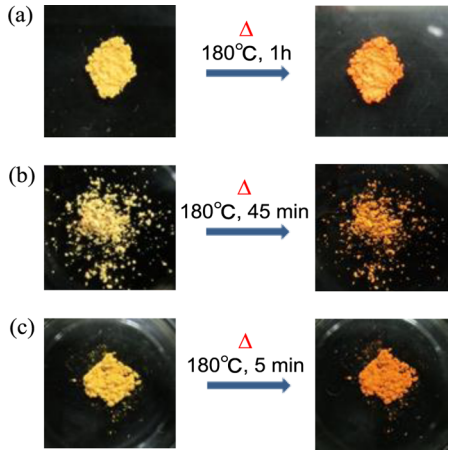

Figure 8. Remarkable change in color of the complexes from yellow to orange by heating in the solid state: (a) thermal conversion from complex **1** to **6**; (b) thermal conversion from complex **2** to **7**; (c) thermal conversion from complex **3** to **8**. The produced orange products of complexes **6**−**8** were confirmed by UV−vis absorption and/or ^{1}H NMR spectra.

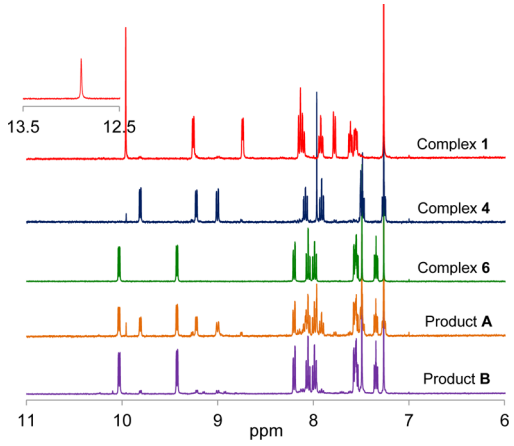

Figure 9. ^{1}H NMR spectra (in $CDCl_3$) of complexes **1** (red line), **4** (blue line), and **6** (green line) and products **A** (orange line) and **B** (purple line) obtained by heating a crystal of complex **1**.

complexes **4** and **6** in a 2:3 molar ratio and those of product **A** fitted very well (Figure S5). On the other hand, the ^{1}H NMR spectrum of product **B** was completely consistent with that of complex **6**. The UV−vis absorption spectra of product **B** were also identical with those of complex **6** (Figure S6). Therefore, coordination structure conversion from complex **1** to complex **6** occurred via complex **4** even in the solid state by heating. It seems that the structure of complex **6** is thermodynamically more stable than that of complex **4**. Considering the structure of complex **1**, the proton attached to N(amide) and the neighboring coordinating chloride ion have a hydrogen-bonding interaction (see above). Therefore, it is expected that the proton and the chloride ion combined quite easily by heating even in the solid to produce HCl vapor. Indeed, we confirmed the evolution of acidic vapor (HCl) from the crystals of complex **1** with pH paper test strips as the structure conversion reaction proceeded by heating. We applied additional experiments. The crystal of complex **1** was heated in the solid state at 120 °C for 1, 2, and 3 h or at 150 °C for 10, 20, and 30 min, and ^{1}H NMR spectra of each product in a $CDCl_3$ solution were measured. We confirmed that all of the

DOI: 10.1021/acs.inorgchem.5b01128
Inorg. Chem. 2015, 54, 8436−8448

samples were mixtures of complexes **1**, **4**, and **6**. After the crystals of complex **1** were heated in the solid state, the ratios of complex **4** and **6** were 2:1 (at 120 °C for 1 h), 5:4 (at 120 °C for 2 and 3 h), and 2:3 (at 150 °C for 10, 20, and 30 min) (Figure S7). Unfortunately, we could not ascertain the optimized condition at which the structure of complex **1** converged to that of complex **4** without producing complex **6**.

TG analysis of the crystal of complex **1** shows that the weight loss of 7.23% at 70−100 °C and then 8.98% at 120−190 °C

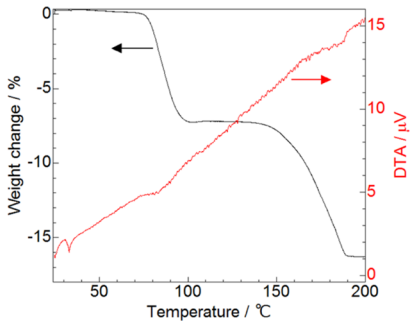

Figure 10. TG analysis of the crystals of complex **1**. Weight loss was observed in a stepwise fashion at 70−100 and 120−190 °C. The former range corresponds to the loss of acetonitrile as solvent molecules of crystallization and the latter to that of HCl vapor produced.

occurred in a stepwise fashion (Figure 10). The single crystal of complex **1** used for X-ray structure determination included acetonitrile as solvent molecules of crystallization. We interpreted the former weight loss as corresponding to the release of acetonitrile molecules included in the crystal of complex **1** and the latter to the HCl vapor produced. The calculated values of the weight loss for the release of acetonitrile and HCl vapor for **1**·CH_3CN were 9.23 and 8.20, respectively. The observed values for the loss of acetonitrile are lower than the expected values because of the efflorescent character of the crystals. The crystals of **1**·CH_3CN gradually lose acetonitrile molecules of crystallization even at room temperature. It is plausible that the sample used for TG analysis was **1**·0.75CH_3CN. The calculated values of the weight loss for the release of CH_3CN and HCl vapor for **1**·0.75CH_3CN (7.09 and 8.39%, respectively) are reasonable to interpret the observed TG analysis data. An additional TG analysis of complexes **1** and **6** was also applied by extending the temperature measuring range up to 400 °C (Figure S8). Each sample decomposed at 250−400 °C, and the weight loss behavior of the complexes at the decomposition temperature range in the TG analyses were extremely similar to each other. These results support that complex **1** was converted to complex **6** upon heating in the solid state.

Similar thermal structure conversion of complex **2** to complex **7** also occurred in the solid state by heating the crystals of complex **2** at 180 °C for 45 min (Figure 8b). The structure conversion reaction of complex **3** in the solid state proceeded faster, at 180 °C for 5 min, to yield complex **8** (Figure 8c). We confirmed that the UV−vis (Figure S9) and ^{1}H NMR spectra (Figure 11) of each orange product (Figure 8b,c) were identical with those of complexes **7** and **8**, respectively. Thus, this structure conversion reaction occurred efficiently not only in solution but also in the solid state by heating. Although the crystals of complexes **6**−**8** were stored

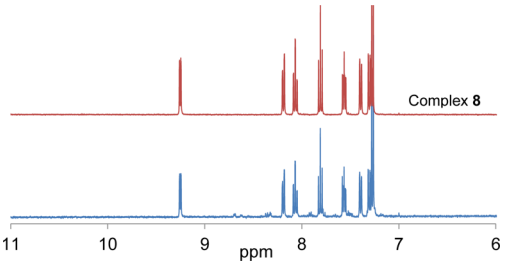

Figure 11. ^{1}H NMR spectra (in $CDCl_3$) of complex **8** (red line) and the orange product (blue line) obtained by heating a crystal of complex **3** at 180 °C for 5 min. A ^{1}H NMR spectrum of poorly soluble complex **3** could not be recorded.

with HCl vapor in closed containers, they did not revert to complexes **1**−**3**.

In contrast, we observed the change in color of the crystals of complexes **4** and **5** from orange to yellow, respectively, by leaving the crystals with HCl vapor in closed containers (Figure 12). The color change occurred rapidly in complex **4** (5 min)

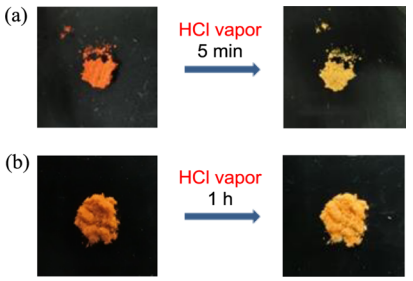

Figure 12. Change in color of the crystals of (a) **4** and (b) **5** from orange to yellow by exposing the crystals to HCl vapor. Complexes **1** and **2** were produced, respectively.

but took longer in complex **5** (ca. 1 h). The UV−vis absorption spectrum of each yellow product was identical with that of complexes **1** and **2** (Figure S10). Accordingly, complexes **4** and **5** reverted to complexes **1** and **2** in the solid state. We believe that the reaction proceeded more slowly in complex **5** because there is a steric hindrance between the methyl group and the O(amide) atom in the produced complex **2**. It is interesting that such substantial thermochromic and vapochromic coordination structure conversions occur even in the solid state.

■ CONCLUSION

In this work, we elucidated that the drastic coordination structure conversion of the hydrazone−palladium(II) complexes occurred not only in solution but also in the solid state. The photochemical and thermal structure conversion reaction caused *E*-to-*Z* isomerization of the coordinating hydrazone ligands. The *κN*(imine) to *κN*(amidate) transformation successfully occurred, and the elimination of hydrazone ligands from the metal accompanied by isomerization was not observed.

We successfully prepared a series of palladium(II) complexes, [$PdCl_2${*κN*(py1),*κN*(imine)-HL^n}] (**1**, n = 1; **2**, n = 2), [$PdCl_2$(*κN*(amidate),*κN*(py2)-HL^n)] (**3**, n = 3), [PdCl{*κN*(py1),*κN*(imine),*κN*(py2)-L^n}] (**4**, n = 1; **5**, n = 2), and [PdCl{*κN*(py1),*κN*(amidate),*κN*(py2)-L^n}] (**6**, n = 1; **7**, n = 2; **8**, n = 3) containing protonated (HL^n) or deprotonated [$(L^n)^-$] hydrazone ligands of HL^n {(*N*′-(pyridin-2-yl)methylene]-picolinohydrazide (HL^1), *N*′-[1-(pyridin-2-yl)ethylidene]-

DOI: 10.1021/acs.inorgchem.5b01128
Inorg. Chem. 2015, 54, 8436−8448

picolinohydrazide (HL^2), and *N*′-[(6-methylpyridin-2-yl)-methylene]picolinohydrazide (HL^3)}. The structures of the complexes were assigned on the basis of X-ray analysis, UV−vis absorption and ^{1}H NMR spectroscopy, and elemental analysis. The molecular and packing structures of **1**·CH_3CN, **2**·CH_3CN, **3**·H_2O, **5**·CH_3CN, **7**·CH_3CN, and **8** were determined by single-crystal X-ray diffraction measurement. The κN(amidate),κN(py2) coordination mode of the HL^3 ligand in complex **3** was different from that of the HL^1 and HL^2 ligands in complexes **1** and **2** [κN(py1),κN(imine)]. Complexes **1**−**3**, in acetonitrile, were thermally converted to complexes **6**−**8**; however, complexes **1** and **2** were transformed into complexes **4** and **5**, respectively, in a basic acetonitrile solution with a small volume of triethylamine at ambient temperature in the dark. We also ascertained that complex **4** reverted to complex **1** in an acidic acetonitrile solution containing a drop of hydrochloric acid by measuring the change in the UV−vis absorption spectra. Complexes **4** and **5** were stable in a basic acetonitrile solution in the dark; however, they photochemically converted to complexes **6** and **7** under room light. Such coordination structure conversions were observed not only in solution but also in the solid state. Complex **1** was transformed to complex **6** via complex **4** by heating the crystals. The evolution of acidic gas (HCl vapor) was confirmed during heating. In addition, complex **4** reverted to complex **1** by exposing the crystals to HCl vapor. We also determined that complex **3** converted to complex **8** by heating the crystals in the solid state. In this study, the coordination structure conversion mechanism and the related chromic properties of several hydrazone−palladium(II) complexes in the solid state and in solution were successfully elucidated by introducing three different hydrazone ligands. It is intriguing that such coordination structure changes occur thermally in an acidic acetonitrile solution and photochemically in a basic acetonitrile solution. There are very few reports on such a large structure conversion of the complexes by exposing the crystals to acidic vapor. Hydrazone ligands have a diverse coordination ability to various kinds of redox-active metal ions. Further investigations focusing on redox reactions of the metal complexes coupled with protonation/deprotonation of the hydrazone ligands are in progress. It will be useful for future application studies in order to develop stimuli-responsive chromic materials.

■ ASSOCIATED CONTENT

Supporting Information

The Supporting Information is available free of charge on the ACS Publications website at DOI: 10.1021/acs.inorgchem.5b01128.

IR spectra of complexes **1**, **4**, **6**, and **2**, **5**, **7**, ^{1}H NMR spectra of complexes **1** and **2** (in CD_3CN) and **4**−**8** (in $CDCl_3$), the drawings of HOMO and LUMO of complexes **5** and **7**, absorption spectrum of complex **4** in a basic acetonitrile solution that includes a small volume of triethylamine, absorption spectra of complex **1** and product **A** in acetonitrile and spectra calculated for a mixture of complexes **4** and **6** in a 4:6 molar ratio, absorption spectra of complex **1**, product **B**, and complex **6** in acetonitrile, ^{1}H NMR spectra of the products obtained from complex **1** on heating at 120 or 150 °C in the solid, TG analysis data of complexes **1** and **6** obtained by extending the temperature measuring range up to 400 °C, absorption spectra of complex **2**, the product obtained by heating the crystal of complex **2** at 180 °C for 45 min, and complex **7** in acetonitrile, absorption spectra of complex **4** and the product obtained by exposing the crystal of complex **4** to HCl vapor for 5 min, and absorption spectra of complex **5** and the product obtained by exposing the crystal of complex **5** to HCl vapor for 1 h (PDF)

X-ray crystallographic data of **1**·CH_3CN (CIF)

X-ray crystallographic data of **2**·CH_3CN (CIF)

X-ray crystallographic data of **3**·H_2O,(CIF)

X-ray crystallographic data of **5**·CH_3CN (CIF)

X-ray crystallographic data of **7**·CH_3CN (CIF)

X-ray crystallographic data of **8** (CIF)

■ AUTHOR INFORMATION

Corresponding Author

*E-mail: knakajim@auecc.aichi-edu.ac.jp.

Notes

The authors declare no competing financial interest.

■ ACKNOWLEDGMENTS

This work was supported by a Grant-in-Aid for Scientific Research Nos. 26410063 and 24550076 from the Ministry of Education, Culture, Sports, Science, and Technology, Japan.

■ REFERENCES

(1) Geldard, J. F.; Lions, F. *Inorg. Chem.* **1963**, *2*, 270−282.

(2) Pal, S.; Pal, S. *J. Chem. Soc., Dalton Trans.* **2002**, 2102−2108.

(3) Pelagatti, P.; Bacchi, A.; Carcelli, M.; Costa, M.; Frühauf, H.-W.; Goubitz, K.; Pelizzi, C.; Triclistri, M.; Vrieze, K. *Eur. J. Inorg. Chem.* **2002**, *2002*, 439−446.

(4) Wood, A.; Aris, W.; Brook, D. J. R. *Inorg. Chem.* **2004**, *43*, 8355−8360.

(5) Dawe, L. N.; Thompson, L. K. *Dalton Trans.* **2008**, 3610−3618.

(6) Raja, D. S.; Bhuvanesh, N. S. P.; Natarajan, K. *Dalton Trans.* **2012**, *41*, 4365−4377.

(7) Guo, Y.-N.; Chen, X.-H.; Xue, S.; Tang. *Inorg. Chem.* **2012**, *51*, 4035−4042.

(8) Huang, W.; Jin, Y.; Wu, D.; Wu, G. *Inorg. Chem.* **2014**, *53*, 73−79.

(9) Franks, A. T.; Peng, D.; Yang, W.; Franz, K. J. *Inorg. Chem.* **2014**, *53*, 1397−1405.

(10) Pelagatti, P.; Bacchi, A.; Carcelli, M.; Costa, M.; Fochi, A.; Ghidini, P.; Leporati, E.; Masi, M.; Pelizzi, C.; Pelizzi, G. *J. Organomet. Chem.* **1999**, *583*, 94−105.

(11) Pelagatti, P.; Bacchi, A.; Balordi, M.; Bolaño, S.; Calbiani, F.; Elviri, L.; Gonsalvi, L.; Pelizzi, C.; Peruzzini, M.; Rogolino, D. *Eur. J. Inorg. Chem.* **2006**, *2006*, 2422−2436.

(12) Pouralimardan, O.; Chamayou, A.-C.; Janiak, C.; Hosseini-Monfared, H. *Inorg. Chim. Acta* **2007**, *360*, 1599−1608.

(13) Carvalho, M. F. N. N.; Fernandes, T. A.; Galvão, A. M.; von Nidda, H.-A. K.; Sampaio, M. A. P. *Inorg. Chim. Acta* **2010**, *363*, 71−76.

(14) Pandiarajan, D.; Ramesh, R. *J. Organomet. Chem.* **2012**, *708*−*709*, 18−24.

(15) Maurya, M. R.; Khurana, S.; Schulzke, C.; Rehder, D. *Eur. J. Inorg. Chem.* **2001**, *2001*, 779−788.

(16) Bernhardt, P. V.; Caldwell, L. M.; Chaston, T. B.; Chin, P.; Richardson, D. R. *JBIC, J. Biol. Inorg. Chem.* **2003**, *8*, 866−880.

(17) Buss, J. L.; Neuzil, J.; Ponka, P. *Arch. Biochem. Biophys.* **2004**, *421*, 1−9.

(18) Rollas, S.; Küçükgüzel, Ş. G. *Molecules* **2007**, *12*, 1910−1939.

(19) Zhang, Y.; Zhang, L.; Liu, L.; Guo, J.; Wu, D.; Xu, G.; Wang, X.; Jia, D. *Inorg. Chim. Acta* **2010**, *363*, 289−293.

(20) Raja, D. S.; Bhuvanesh, N. S. P.; Natarajan, K. *Dalton Trans.* **2012**, *41*, 4365−4377.

DOI: 10.1021/acs.inorgchem.5b01128
Inorg. Chem. 2015, 54, 8436−8448

(21) Alagesan, M.; Bhuvanesh, N. S. P.; Dharmaraj, N. *Dalton Trans.* **2013**, *42*, 7210−7223.
(22) Anwar, M. U.; Tandon, S. S.; Dawe, L. N.; Habib, F.; Murugesu, M.; Thompson, L. K. *Inorg. Chem.* **2012**, *51*, 1028−1034.
(23) Chandrasekhar, V.; Hossain, S.; Das, S.; Biswas, S.; Sutter, J.-P. *Inorg. Chem.* **2013**, *52*, 6346−6353.
(24) Adhikary, A.; Sheikh, J. A.; Biswas, S.; Konar, S. *Dalton Trans.* **2014**, *43*, 9334−9343.
(25) Bakir, M.; Green, O. *J. Mol. Struct.* **2011**, *996*, 24−30.
(26) Vantomme, G.; Lehn, J.-M. *Angew. Chem., Int. Ed.* **2013**, *52*, 3940−3943.
(27) Chang, M.; Horiki, H.; Nakajima, K.; Kobayashi, A.; Chang, H.-C.; Kato, M. *Bull. Chem. Soc. Jpn.* **2010**, *83*, 905−910.
(28) Chang, M.; Kobayashi, A.; Chang, H.-C.; Nakajima, K.; Kato, M. *Chem. Lett.* **2011**, *40*, 1335−1337.
(29) Mori, A.; Suzuki, T.; Sunatsuki, Y.; Kojima, M.; Nakajima, K. *Bull. Chem. Soc. Jpn.* **2015**, *88*, 480−489.
(30) Mori, A.; Suzuki, T.; Sunatsuki, Y.; Kobayashi, A.; Kato, M.; Kojima, M.; Nakajima, K. *Eur. J. Inorg. Chem.* **2014**, *2014*, 186−197.
(31) Kobayashi, A.; Dosen, M.; Chang, M.; Nakajima, K.; Noro, S.; Kato, M. *J. Am. Chem. Soc.* **2010**, *132*, 15286−15298.
(32) Chang, M.; Kobayashi, A.; Nakajima, K.; Chang, H.-C.; Kato, M. *Inorg. Chem.* **2011**, *50*, 8308−8317.
(33) Yamashita, Y.; Tateishi, T.; Sawaguchi, K.; Kobayashi, A.; Kato, M.; Nakajima, K. *Chem. Lett.* **2014**, *43*, 1912−1914.
(34) Nonoyama, M. *Inorg. Chim. Acta* **1974**, *10*, 133−137.
(35) Drew, D.; Doyle, J. R. *Inorg. Synth.* **1972**, *13*, 52−53.
(36) Doyle, J. R.; Slade, P. E.; Jonassen, H. B. *Inorg. Synth.* **1960**, *6*, 218−219.
(37) *RAPID AUTO*, version 2.30; Rigaku Corp.: Tokyo, Japan; 2005.
(38) *CrystalClear*, version 1.4.0; Rigaku Corp.: Tokyo, Japan; 2008.
(39) *SIR2004*: Burla, M. C.; Caliandro, R.; Camalli, M.; Carrozzini, B.; Cascarano, G. L.; De Caro, L.; Giacovazzo, C.; Polidori, G.; Spagna, R. *J. Appl. Crystallogr.* **2005**, *38*, 381−388.
(40) *SHELX97*: Sheldrick, G. M. *Acta Crystallogr., Sect. A: Found. Crystallogr.* **2008**, *64*, 112−122.
(41) *CrystalStructure, Version 4.1: Crystal Structure Analysis Package*; Rigaku Corp.: Tokyo, Japan, 2014.
(42) Padwa, A. *Chem. Rev.* **1977**, *77*, 37−68.
(43) Becker, R. S.; Chagneau, F. *J. Am. Chem. Soc.* **1992**, *114*, 1373−1381.
(44) Chaur, M. N.; Collado, D.; Lehn, J.-M. *Chem. - Eur. J.* **2011**, *17*, 248−258.
(45) Vantomme, G.; Lehn, J.-M. *Angew. Chem., Int. Ed.* **2013**, *52*, 3940−3943.
(46) Yamada, T.; Maruta, G.; Takeda, S. *Chem. Commun.* **2011**, *47*, 653−655.

DOI: 10.1021/acs.inorgchem.5b01128
Inorg. Chem. 2015, 54, 8436−8448